

## Supporting Information

### Formation of Protocell-like Vesicles in a Thermal Diffusion Column

Itay Budin<sup>†§</sup>, Raphael J. Bruckner<sup>‡§</sup>, and Jack W. Szostak<sup>§</sup>

<sup>†</sup>Department of Molecular and Cellular Biology, Harvard University, Cambridge, MA 02138,

<sup>‡</sup>Department of Genetics, Harvard Medical School, Boston, MA 02115, and <sup>§</sup>Howard Hughes Medical Institute, Department of Molecular Biology and the Center for Computational and Integrative Biology, Massachusetts General Hospital, Boston, MA 02114

This file includes Materials and Methods, Text S1-S2 with references, Table S1 with references, Figures S1-S5, and Movie S1.

#### Materials and Methods

**Thermal diffusion columns:** Borosilicate microcapillaries (VitroCom, Mountain Lakes, NJ) with a square cross section (ID 200  $\mu\text{m}$ , OD 400  $\mu\text{m}$ ) were cut to ~3 cm and sealed via microforge (Narishige, Japan). Bent capillaries were cut to ~4 cm, shaped over an open flame, with a 90° corner 3 cm from the top, and sealed with epoxy. All capillaries were attached to 100-200  $\mu\text{L}$  reservoirs with epoxy. Linear capillaries were loaded with the starting solution via centrifugation (2000 rpm for 15 minutes in a custom built holder). Bent capillaries were loaded by pipette before being sealed.

**Thermal gradient:** Capillaries with attached reservoirs were loaded with an initial solution and clamped between a heat source and sink in a custom built apparatus. The heat source block was attached to a high performance hot plate (IKA, Wilmington, NC) to maintain a constant temperature, which was monitored by a temperature probe attached to the block. The sink was cooled by coolant circulation from a ultra-low temperature cold bath (Thermo Scientific, Waltham, MA). Since the insulating glass walls of the capillary were relatively thick, the temperature gradient across the solution was significantly lower than that between the hot and cold blocks. Therefore temperature gradients across the solution ( $\Delta T$ ) were calculated by modeling steady state heat conduction across a composite slab (1). Taking the heat flux across the solution as equal to the total heat flux:

$$\left(\frac{\Delta T}{k_w}\right) = \left(\frac{T_H - T_C}{\frac{OD - ID}{k_g} + \frac{ID}{k_w}}\right)$$

Where  $T_H$  and  $T_C$  are the heat sink temperatures and  $k_w$  and  $k_g$  are the thermal conductivities for water (0.6 W/mK) and borosilicate glass (1.13 W/mK). Solving for the temperature difference across the solution:

$$\Delta T = \frac{ID(T_H - T_C)}{\frac{k_w}{k_g}(OD - ID) + ID}$$

Since  $ID = (OD - ID) = 200 \mu\text{m}$

$$\Delta T = \frac{T_H - T_C}{\frac{k_w}{k_g} + 1}$$

Therefore, for a  $\Delta T$  of 30 K, we set  $T_H - T_C = 45$ ; the heat source was kept at 50° C and the sink at 5° C.

**Solutions:** Oleate (Nu-chek Prep, Eugene, OR) solutions were prepared either by evaporation and rehydration of a stock solution in methanol, or by dilution of an 80  $\mu$ M stock solution in buffer. Unless otherwise noted, all oleate solutions were buffered by 0.2 M Bicine (Sigma-Aldrich, St. Luis, MO), titrated with NaOH to pH 8.5. Bulk vesicle preparations were made by dissolving oleate in buffer followed by gentle shaking overnight. For fluorescence accumulation experiments, the following solutes were used: HPTS (Sigma-Aldrich), 20 bp poly-A DNA with a 5' carboxyfluorescein modification (Integrated DNA Technologies, Coralville, IA), and Cy3-dCTP (GE Biosciences, Britain). For bilayer staining experiments, Rhodamine 6G (Sigma-Aldrich) was included in the vesicle solution at 2 nM.

**Capillary imaging:** Capillaries were viewed with a Nikon TE2000S inverted epifluorescence microscope with extra long working distance (ELWD) objective lenses. The illumination source was either a bright field lamp through a phase contrast filter (Nikon) or a metal halide lamp (EXFO, Canada) with a  $480 \pm 20$  nm (for HPTS and labeled oligomers) or a  $546 \pm 5$  nm (for Cy3-dCTP and Rhodamine staining) optical filter. Fluorescence emission was filtered either at  $535 \pm 25$  nm (for HPTS and labeled oligomers) or 590 nm long pass (for Cy3-dCTP and Rhodamine staining). Images were taken with a CCD camera (Hamamatsu Photonics, Japan) and processed with commercial software (Phylum Live, Lexington, MA and ImageJ, NIH). Fluorescence was quantified using the image analysis software ImageJ and normalized to the

corresponding value for the initial starting solution. Standard curves for fluorescent solutes were used to ensure that fluorescence was linearly dependent on concentration in the ranges used.

**Capillary streamline visualization:** Dye-labeled (Dragon Green) 1.90  $\mu\text{m}$  microspheres (Bangs Laboratories, Fishers, IN) were diluted 100-fold in a 1:1 solution of water and deuterium oxide (final density = 1.05 g/mL). The capillary was loaded with this solution and imaged with a CMOS camera (Vision Research, Wayne, NJ) connected to an ELWD 10x objective (Nikon) through an InfiniTube (Infinity, Boulder, CO). The microspheres were illuminated with a hand-held UV lamp that was directed orthogonally to the camera path.

**Oleate accumulation:**  $^3\text{H}$ -Oleate (Moravek Biochemicals, Brea, CA) in methanol was evaporated and resuspended in water with one mole equivalent of NaOH. The resulting solution of labeled micelles was loaded into a linear capillary and subjected to a temperature gradient for 24 hours. The capillary was then fractionated into 0.75 cm lengths using forceps and a wire cutter. Fractions were crushed in 100  $\mu\text{L}$  water to disperse the solution and centrifuged to remove the glass (12,000 RPM for 10 minutes). The supernatant was then added to 2 mL of scintillation cocktail (MP Biomedicals, Costa Mesa, CA). Counts were read using a Beckman Coulter LS6500 scintillation counter and normalized to values taken from an equivalent volume of 60  $\mu\text{M}$   $^3\text{H}$ -oleate.

**Vesicle imaging:** Vesicle cargo encapsulation was visualized by gently replacing the buffer in the capillary with dye-free buffer. The sealed bottom of the capillary was first snapped off and the reservoir was loaded with a buffered solution of 80  $\mu\text{M}$  oleate (equal to the cac; to prevent

vesicle dissolution). The dye-free buffer was then allowed to flow through the capillary by gravity until  $> 2$  mL of buffer ( $\sim 1000$  times the capillary volume) had flowed through.

Alternatively, cargo-free vesicles and bulk vesicle preparations were visualized with Rhodamine 6G membrane staining.

### **Text S1: Analysis of solute transport into a microcapillary**

On our experimental time scale (24-48 hours), concentration was achieved primarily by local redistribution of the initial solute in the capillary, not by accumulation of solute from the reservoir. Therefore, regions of the capillary near the top were almost completely depleted of solute. This significantly limited the absolute concentration that could be achieved in our capillaries: while we were able to achieve concentration gradients (bottom/top final concentrations) of over 1000 fold, the absolute concentration at the bottom of the capillary was only  $\sim 10$  fold higher than the initial concentration. However, over much longer times, we would expect continued diffusion of solute from the reservoir into the capillary to result in much higher solute concentrations at the bottom of the capillary, assuming a dilute starting solution. Therefore, although vesicle formation in our experiments was limited to initial oleate concentrations  $> 30 \mu\text{M}$ , over long time scales we expect that sub- $\mu\text{M}$  initial concentrations would still allow oleate to accumulate to concentrations above the cac.

This technical limitation of our experimental system was due to the slow diffusion of molecules from the reservoir into the top of the capillary, at which point they could enter the convective flow. There was a gap of ~0.5 cm between the reservoir and the onset of the thermal gradient in the capillary across which the solute (DNA nucleotide and oligomer, oleate micelle) from the reservoir had to diffuse. We can model this transport as a one-dimensional diffusive flux at steady state:

$$J_{A,x} = D \cdot A \cdot \frac{dC}{dx} = D \cdot A \cdot \frac{C_{\text{reservoir}} - C_{\text{capillary,top}}}{d_{\text{res,cap}}}$$

where A is the cross sectional area of the capillary and  $d_{\text{res,cap}}$  is the distance from the reservoir to the capillary (~0.5 cm). D is the molecular diffusion coefficient:  $4 \times 10^{-6}$  cm<sup>2</sup>/s for a single nucleotide (S2),  $10^{-6}$  cm<sup>2</sup>/s for an ~20mer oligonucleotide (S2), and  $2.8 \times 10^{-6}$  cm<sup>2</sup>/s for an oleate micelle (S3). Taking the top concentration as ~0 (totally depleted) and the reservoir concentration at 40  $\mu$ M, the flux from the reservoir into the capillary was 11 picomoles/day of the single nucleotides, 7 picomoles/day of the 20mer, and 20 picomoles/day of oleate. That represents 23%, 6%, and 12%, respectively, of the initial solute in the capillaries. Therefore, over the time course of our experiments (~24 hours), the amount of a new solute diffusing from the reservoir into the capillary was small compared to the amount of solute that was initially loaded into the capillary.

## **Text S2: Description and analysis of vesicle formation**

Unexpectedly, the vesicles that formed in the bent capillaries were quite large: up to ~6  $\mu$ m, with their size dependent on the starting oleate concentration (Figure S4). They assembled in discrete, adherent populations, with a surprising degree of size uniformity. As expected, the number of

vesicles was significantly increased by using a low salt buffer, likely due to increased oleate accumulation (Figure S5). Because of the diffusion limitation discussed above, the concentration of oleate was largely limited by the redistribution of the oleate within the capillary itself. Therefore, if we assume all of the oleate in the capillary was concentrated into the extruded portion, the maximum oleate concentration was  $\sim 280 \mu\text{M}$  for a starting concentration of  $70 \mu\text{M}$ . Concentrations in this range form far smaller vesicles in bulk preparations (Figure S4C). Higher concentration solutions, which can form large vesicles, produce highly polydisperse populations (Figure S4D).

We attribute these unusual features to the mechanism by which the vesicles formed in our experiments. The fatty acid accumulation in the capillary extended into the protruding segment, where the convective flow is blocked by the geometry and absence of the temperature gradient. Here, nascent vesicles were able to nucleate in the absence of convective flow. As fatty acids continued to concentrate, they preferentially incorporated into the pre-formed vesicles instead of nucleating newer vesicles, a kinetically slower process (S4). Our group has previously noticed that when adding micelles to a buffered vesicle solution, the efficiency of vesicle growth (as opposed to new vesicle nucleation) increases with lower micelle addition rates (S4). Here, the thermal diffusion column accumulates low concentrations of fatty acids extremely slowly (over the course of hours), which would strongly favor growth of existing vesicles over the nucleation of new vesicles. Thus, an initial population of small nascent vesicles all underwent similar growth by the incorporation of continuously accumulating fatty acids. This led to a relatively small number of large monodisperse vesicles. The adherence of the vesicles could have further assisted vesicle survival by preventing diffusion back into the convective flow. However, the

surface adsorption of the vesicles was not permanent; a small portion of the large vesicles could be seen to exhibit Brownian motion (and were thus detached from the glass) in our experiments. Extended incubation at room temperature led to additional vesicles detaching into the solution.

It is also important to note that vesicle formation is not specific to the geometry we used, but rather would be promoted by any method of disrupting the convective flow from running along the concentration gradient. For example, we observed vesicles in linear capillaries in which there were unintended blockages of the convective flow due to a large particle or an air bubble.

Another possible approach is altering the diameter of the capillaries to allow for the thermophoretic trapping of newly formed vesicles, thereby preventing them from flowing back into the low concentration region. Capillaries with narrower diameters are predicted to more efficiently concentrate large, aggregate structures, such as vesicles (S2). However, a narrower capillary would also be less efficient at concentrating fatty acids below the cac, which are present as more diffusive monomers and micelles. Thus, lipid polymorphism represents a unique problem for thermal accumulation, which we were able to circumvent by geometrically disrupting the convective flow. An alternative approach might be to use capillaries with variable diameters, so that dilute fatty acids are efficiently concentrated and newly formed vesicles remain thermophoretically trapped in the high concentration region.

## Table S1

**Table 1:** Approximate critical aggregation concentrations (cac) for prebiotically relevant lipids.

Decanoic acid (C10)	Myristoleic acid (C14:1)	Myristoleic acid with monomyristolein (2:1)	Palmitoleic acid (C16:1)	Oleic acid (C18:1)	Phospholipids
100 mM <sup>5</sup>	4 mM <sup>6</sup>	1 mM <sup>7</sup>	250 μM <sup>8</sup>	80 μM <sup>9</sup>	< 10 nM <sup>10</sup>

## Figures S1-S5

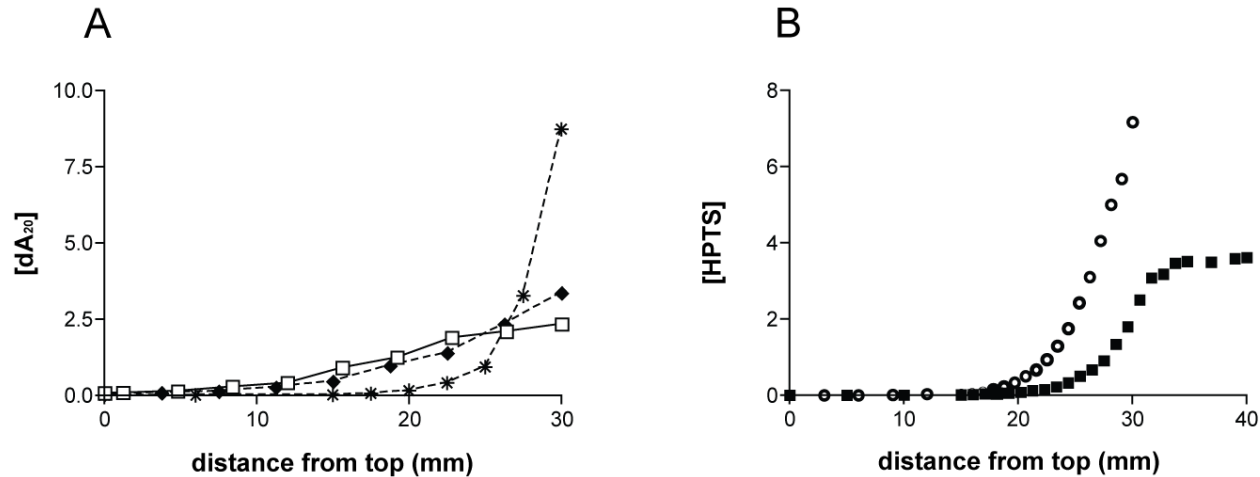


**Figure S1.** Effect of salt concentration and capillary geometry on concentration in thermal diffusion columns. (A) Redistribution of fluorescently labeled DNA 20mer in 3 cm linear capillaries incubated at  $\Delta T = 30$  K for 24 hours. Individual experiments were performed at 10 mM Tris 7.5 with (\*) no added salt (◆) 100 mM NaCl and (□) 250 mM NaCl (connecting lines added for clarity). (B) Effect of capillary geometry on concentration of HPTS at  $\Delta T = 30$  K for 24 hours in 10 mM Tris 7.5. (●) Linear capillary (3 cm length) (■) Bent capillary with a 3 cm vertical length and a 1 cm isothermal orthogonal protrusion. Accumulation extends into and is kept constant in the protruding portion (30-40 mm). All concentrations normalized to the initial solute concentration in the capillary before incubation.

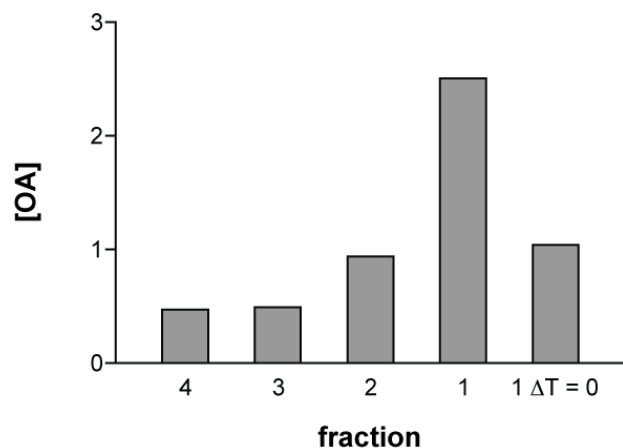


**Figure S2.** Microcapillary thermal diffusion column concentrates oleic acid.  $60 \mu\text{M}$   $^3\text{H}$  oleate at pH 11 after 24 hours was run in a linear microcapillary at  $\Delta T = 30 \text{ K}$ . The capillary was fractionated (300 nL each) and oleate concentration was measured by liquid scintillation counting. The top fraction (1) contained a  $> 5$  fold increase in concentration over the bottom fraction (4), a 2.5 fold increase over the initial concentration. Fractions in capillaries incubated isothermally ( $\Delta T = 0$ ) showed no accumulation. Oleate concentrations normalized to the initial concentration in the capillary before incubation.

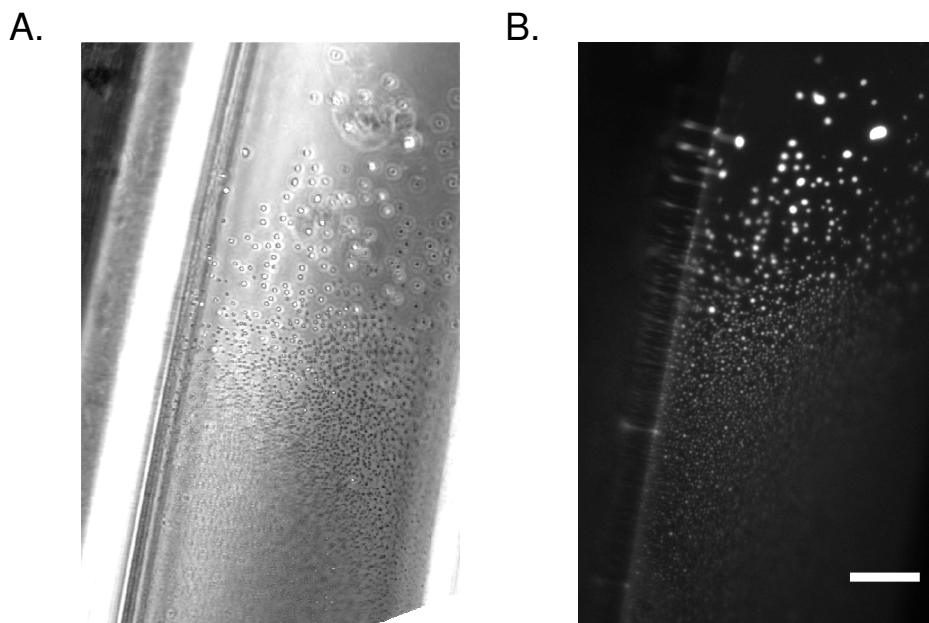


**Figure S3.** Vesicles formed in thermal diffusion column can encapsulate nucleic acids. (A) Phase contrast and (B) epifluorescence image of  $50 \mu\text{M}$  oleic acid incubated at  $\Delta T = 30 \text{ K}$  for 48 hours.  $1 \text{ mM}$  of fluorescein-tagged DNA oligonucleotides (poly-A 20mer) was also included in the starting solution and was co-concentrated with the oleic acid. Non-encapsulated DNA was washed away after incubation, leaving only encapsulated cargo to be visualized. Scale bar =  $60 \mu\text{m}$ .

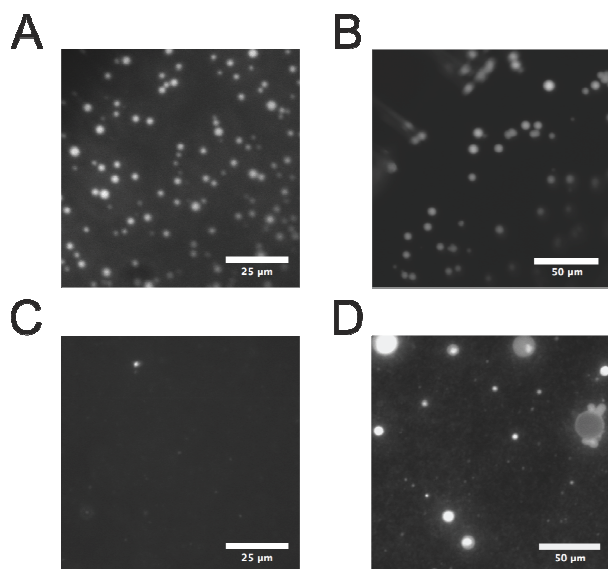


**Figure S4.** Vesicles formed in bent capillaries are large and monodisperse relative to those formed in bulk solution. (A) Oleic acid vesicles formed in a capillary with a starting fatty acid concentration of 40  $\mu\text{M}$  and (B) 70  $\mu\text{M}$ . In comparison, vesicles formed in bulk at (C) 250  $\mu\text{M}$  are mostly too small to see and at (D) 25 mM are polydisperse (diluted 1:10 after vesicle formation for visual clarity). All vesicles stained with the membrane dye Rhodamine 6G.

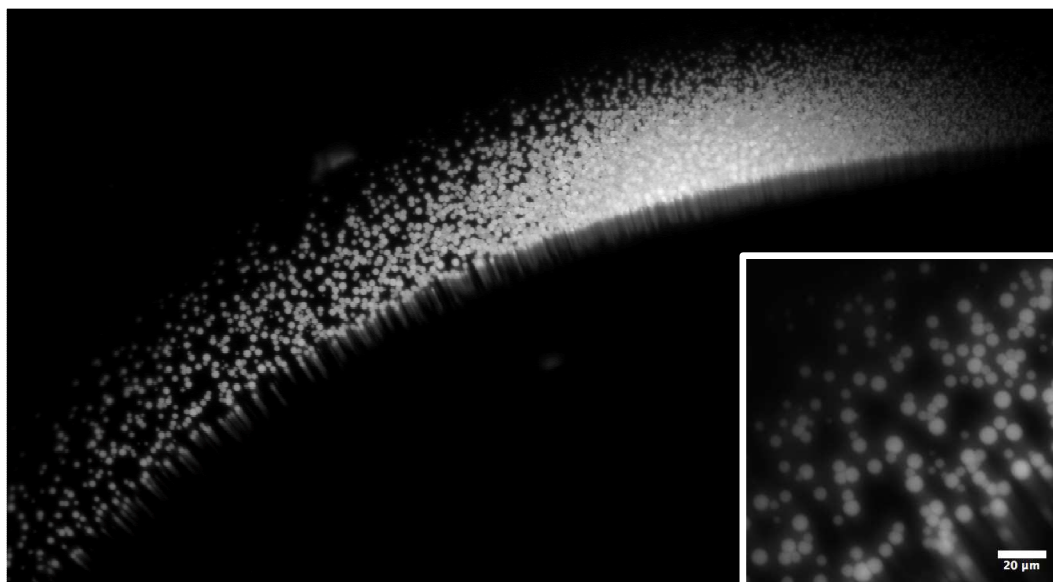


**Figure S5.** Vesicle formation in a bent capillary under a low salt concentration. Oleic acid (60  $\mu\text{M}$ ) was incubated at  $\Delta T = 30\text{K}$  for 48 hours in 20 mM  $\text{Na}^+\text{Bicine}$  pH 8.5. Compared to similar experiments performed at 0.2 M  $\text{Na}^+$  (Figure 2), a significant enhancement in the number of assembled vesicles is demonstrated. Insert: close-up of vesicles from same image. Vesicles stained with the membrane dye Rhodamine 6G.

## Movie S1

Example of the convective flow in a microcapillary (200  $\mu\text{m}$  ID) under a lateral thermal gradient of 30 K (left wall is cooled, right wall is heated). Flow is visualized with dye-labeled polystyrene beads and is shown at 30x speed.

## References

- (1) Datta, A.K. *Biological and Bioenvironmental Heat and Mass Transfer*. Marcel Dekker: New York, 2002, 240-2.
- (2) Baaske, P.; Weinert, F.M.; Duhr, S.; Lemke, K.H.; Russell, M.J.; Braun, D. *Proc. Natl. Acad. Sci. USA*. **2007**, 104, 9346-51.
- (3) Stewart, J.M.; Driedzic, W.R.; Berkelaar, J.A. *Biochem. J.* **1991**, 275, 569-73.
- (4) Chen, I.A.; Szostak, J.W. *Biophys. J.* **2004**, 87, 988-98.
- (5) Mansy, S.S.; Schrum, J.P.; Krishnamurthy, M.; Tobé, S.; Treco, D.A.; Szostak, J.W. *Nature* **2008**, 454, 122-5.
- (6) Hanczyc, M.M.; Fujikawa, S.M.; Szostak, J.W. *Science* **2003**, 302, 618-22.
- (7) Chen, I.A.; Szostak, J.W. *Science* **2004**, 305, 1474-6.
- (8) Measured by Dynamic Light Scattering as described in S9.
- (9) Chen, I.A.; Szostak, J.W. *Proc. Natl. Acad. Sci. USA*. **2004**, 101, 7965-70.
- (10) Abreu, M.S.; Moreno, M.J.; Vaz, W.L. *Biophys. J.* **2004**, 87, 353-65.